International Journal of Modern Physics E
© World Scientific Publishing Company

Parametrization of Bose-Einstein Correlations in e^+e^- Annihilation and Reconstruction of the Source Function

W.J. Metzger, T. Novák, T. Csörgő,* and W. Kittel
for the L3 Collaboration
w.metzger@hef.ru.nl
Radboud University, Toernooiveld 1, 6525 ED Nijmegen, The Netherlands

Received (received date)
Revised (revised date)

A short review of Bose-Einstein correlations in hadronic e^+e^- annihilation is presented. Bose-Einstein correlations of pairs of identical charged pions in hadronic Z-boson decays are analyzed in terms of various parametrizations. A good description is achieved using a Lévy stable distribution in conjunction with a hadronization model having highly correlated configuration and momentum space, the τ-model. Using these results, the source function is reconstructed.

1. Introduction

In particle and nuclear physics, intensity interferometry provides a direct experimental method for the determination of sizes, shapes and lifetimes of particle-emitting sources (for reviews see, *e.g.*, Refs. 1–5). In particular, boson interferometry provides a powerful tool for the investigation of the space-time structure of particle production processes, since Bose-Einstein correlations (BEC) of two identical bosons reflect both geometrical and dynamical properties of the particle radiating source.

After a brief review of some results on BEC in e^+e^- annihilation, we present new results from the L3 Collaboration on BEC in hadronic Z decay. We investigate various static parametrizations in terms of the four-momentum difference, $Q = \sqrt{-(p_1 - p_2)^2}$ and find that none give an adequate description of the Bose-Einstein correlation function. However, within the framework of models assuming strongly correlated coordinate and momentum space a good description is achieved. Using this description, the complete space-time picture of the particle emitting source in hadronic Z-boson decay is reconstructed.

*Visitor from Budapest, Hungary, sponsored by the Scientific Exchange between Hungary (OTKA) and The Netherlands (NWO), project B64-27/N25186.

2. Review of some BEC results in e^+e^- annihilation

The correlation function of q particles with four-momenta p_1, p_2, ..., p_q is given by the ratio of the two-particle number density, $\rho_q(p_1, ..., p_q)$, to the product of the single-particle number densities, $\rho_1(p_1)...\rho_1(p_q)$. Since we are here interested only in the correlation due to Bose-Einstein interference, the product of single-particle densities is replaced by $\rho_{0q}(p_1, ..., p_q)$, the q-particle density that would occur in the absence of BEC. Since the mass of the q identical particles is fixed, the Bose-Einstein correlation function, R_q, is defined in $3q$-dimensional momentum space. It is usually regarded as a function of Q, where $Q^2 = M_q^2 - (qm)^2$ with M_q the mass of the q particles and m the mass of each particle. If the particles have identical four-momenta, $Q = 0$.

In this paper we restrict ourselves to 2-particle BEC. In that case, Q^2 is simply the four-momentum difference, $Q = \sqrt{-(p_1 - p_2)^2}$, and the Bose-Einstein correlation function is given by

$$R_2(p_1, p_2) = \frac{\rho_2(p_1, p_2)}{\rho_0(p_1, p_2)} \tag{1}$$

$$R_2(Q) = \frac{\rho_2(Q)}{\rho_0(Q)} \ , \tag{2}$$

where we write simply ρ_0 instead of ρ_{02}.

It can be shown in a variety of ways that R_q is related to the spatial distribution of the particle production.[2,6] For example, assuming incoherent particle production and a spatial source density of pion emitters, $S(x)$, leads to $R_2(Q) = 1 + |G(Q)|^2$, where $G(Q) = \int \mathrm{d}x\, e^{iQx} S(x) = |G|\, e^{i\phi}$ is the Fourier transform of $S(x)$. Assuming $S(x)$ to be a Gaussian with radius r results in

$$R_2(Q) = 1 + \lambda e^{-Q^2 r^2} \ , \tag{3}$$

where we have inserted, as is customary, an additional parameter, λ, which is meant to account for several effects such as partial coherence (completely coherent particle production would imply $\lambda = 0$), multiple sources and particle purity.

The lack of time dependence in S is certainly wrong. The assumption of a spherical Gaussian distribution of particle emitters may seem unlikely in e^+e^- annihilation, where there is a definite jet structure. However, we must keep in mind that BEC only occur among particles produced close to each other in phase space. Thus, success of (3) in describing the data does not imply that the hadronization volume is a sphere of radius r.

Other parametrizations have been considered in the literature. Nevertheless, in spite of the above-noted limitations, this Gaussian parametrization (3) is most frequently used by experimentalists. When it does not fit well, an expansion about the Gaussian (Edgeworth expansion[7]) can be used instead. Clearly, results can be compared only if the same parametrization is used.

2.1. *Experimental Difficulties*

There are several experimental problems affecting BEC results and their interpretation. Particle purity, resonances and weak decays all affect the measured values of λ and r. For example, in hadronic Z decay about 15% of the charged particles are not pions and about 84% of charged pions are produced via resonances. Other problems are the effect of final-state interactions, both Coulomb and strong, and the choice of the "reference sample," the sample for which ρ_0 is the density. For a discussion of these problems, see, *e.g.*, Ref. 8. Finally, there is the effect of long-range correlations not adequately taken into account by the reference sample. R_2 is not usually found to be constant at large Q. To account for this the right hand side of (3) is multiplied by an appropriate factor, usually a linear dependence on Q: $\gamma\,(1+\delta Q)$.

2.2. *Experimental Results*

2.3. *Dependence on the reference sample*

The values of λ and r found for charged-pion pairs from hadronic Z decays by ALEPH,[9,10] DELPHI,[11] L3[12] and OPAL[13–15] are displayed in Fig. 1. Solid points are corrected for pion purity; open points are not. This correction increases the value of λ but has little effect on the value of r. All of the results with $r > 0.7$ fm were obtained using an unlike-sign reference sample, while those with smaller r were obtained with a mixed reference sample. The choice of reference sample clearly has a large effect on the observed values of λ and r. In comparing results we must therefore be sure that the reference samples used are comparable.

2.4. *Dependence on the center-of-mass energy*

Comparison of values of r obtained using the same reference sample for $\sqrt{s} = 29$–91 GeV shows no evidence of a $\sqrt{s}$ dependence,[8] as seen in Fig. 1.

2.5. *Dependence on the particle mass*

It has been suggested, on several grounds,[20] that r should depend on the particle mass as $r \propto 1/\sqrt{m}$. Values of r found at LEP for various types of particle are shown in Fig. 1. Comparing only results using the same type of reference sample (in this case mixed), we see no evidence for a $1/\sqrt{m}$ dependence. Rather, the data suggest one value of r for mesons and a smaller value for baryons. The value for baryons, about 0.1 fm, seems very small; if true it is telling us something unexpected about the mechanism of baryon production. However, Gustafson has suggested that such a conclusion is premature,[21] since the baryon results rely strongly on comparisons with Monte Carlo and the uncertainties in the Monte Carlo implementation of baryon production are large.

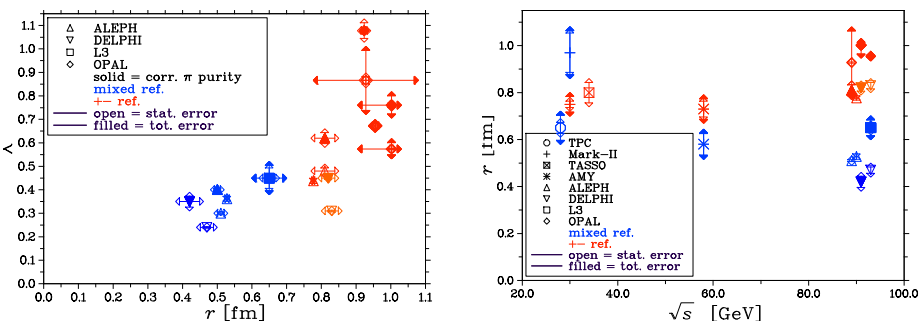

Fig. 1. (left) λ and r at $\sqrt{s} = M_Z$ found in the LEP experiments.[9–15] (right) Dependence of r on the center-of-mass energy from 2-particle BEC for charged pions,[9–19] For clarity some points are shifted slightly in $\sqrt{s}$.

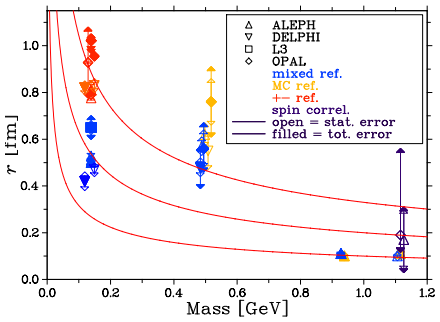

Fig. 2. Dependence of r on the mass of the particle as determined at $\sqrt{s} = M_Z$ from 2-particle BEC for charged pions,[9–15] charged kaons[22,23] and neutral kaons[22,24,25] and from Fermi-Dirac correlations for protons[24] and lambdas.[26,27] The curves illustrate a $1/\sqrt{m}$ dependence.

2.6. *Elongation of the source*

The Gaussian parametrization (3) assumes a spherical source. Given the jet structure of e^+e^- events, one might expect a more ellipsoidal shape. String models predict such a shape with the longitudinal (along the jet axis) radius being longer than the transverse radii.[28–30]

To investigate this, the parametrization is generalized to allow different radii along and perpendicular to the jet axis. The analysis uses the longitudinal center-of-mass system (LCMS). The LCMS system is defined in the following way: The pion pair is boosted along the jet-axis (*e.g.*, the thrust axis), to a frame where the sum of the longitudinal momenta of the two pions is zero. The transverse axes, called "out" and "side" are defined such that the out direction is along the vector sum of the two pion momenta, $\vec{p}_1 + \vec{p}_2$, and the side direction completes the Cartesian coordinate frame. The advantage of the LCMS is that the energy difference, and therefore the difference in emission time of the pions, couples only to the out-component,

$Q_{\rm out}$. Thus $Q_{\rm L}$ and $Q_{\rm side}$ reflect only spatial dimensions of the source, while $Q_{\rm out}$ reflects a mixture of spatial and temporal dimensions. Three-dimensional analyses parametrizing R_2 as a function of $Q_{\rm L}$, $Q_{\rm side}$, and $Q_{\rm out}$ have been performed by L3[31] and OPAL.[15] The longitudal radius, $r_{\rm L}$, is found to be about 20% larger than the side (transverse) radius, $r_{\rm side}$. Further, the amount of the elongation increases when narrower 2-jet events are selected.[15]

On the other hand, ALEPH[10] and DELPHI[32] have restricted themselves to two-dimensional analyses, in which the out and side components are replaced by a transverse one, $Q_{\rm t}^2 = Q_{\rm out}^2 + Q_{\rm side}^2$. This has the disadvantage that the interpretation of the corresponding parameter, $r_{\rm t}$, as a transverse radius is not unambiguous, since it includes the effect of the difference in emission time. Nevertheless, both experiments find the transverse radius smaller than the longitudinal one.

It should also be mentioned that ZEUS performed a similar 2-dimensional analysis in deep inelastic ep interactions.[33] The ratio $r_{\rm t}/r_{\rm L}$ found is similar to that found by DELPHI and ALEPH and is independent of the virtuality of the exchanged photon.

2.7. *Dependence on the transverse mass*

There have been reports that the radius, r, found in 2-pion BEC depends on the average transverse mass of the pions.[34,35] The results of these analyses in the LCMS are shown in Fig. 3. The radii decrease with $m_{\rm t}$, approximately as $r = a + b/\sqrt{m_{\rm t}}$.

2.8. *Conclusions*

The study of BEC in e^+e^- presents a number of problems, both experimental and theoretical. Values obtained for parameters vary considerably among experiments, even when the same parametrization is used. Nevertheless, certain features are clear: BEC exist; they seem independent of cms energy; and the source shape is somewhat elongated in the jet direction. Additionally, the (Fermi-Dirac) radius for baryons may be smaller than the radius for mesons, and there is some evidence that the radius decreases with increasing transverse mass of the pions.

3. New Analysis

We now turn to a new analysis of BEC in hadronic Z decay. We investigate various static parametrizations in terms of the four-momentum difference, Q, and find that none give an adequate description of the Bose-Einstein correlation function. However, within the framework of models assuming strongly correlated coordinate and momentum space a good description is achieved, which is then used to reconstruct the complete space-time picture of the particle emitting source in hadronic Z-boson decay.

The data used in the analysis were collected by the L3 detector[36–40] at an e^+e^- center-of-mass energy of $\sqrt{s} \simeq 91.2$ GeV. Approximately 36 million like-sign pairs of well-measured charged tracks of about 0.8 million hadronic Z decays are used.[41]

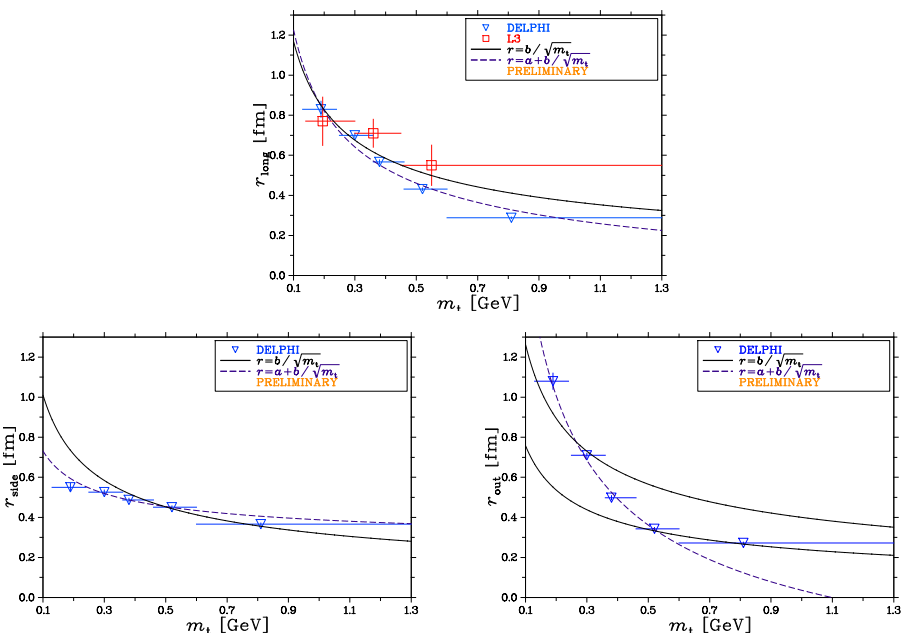

Fig. 3. Dependence of r on the average transverse mass of the pions as determined at $\sqrt{s} = M_Z$ from 2-particle BEC for charged pions.[34,35] The curves illustrate a $r = a + b/\sqrt{m_t}$ or $r = b/\sqrt{m_t}$ dependence.

We perform analyses on the complete sample as well as on two- and three-jet samples. The latter are found using calorimeter clusters with the Durham jet algorithm[42–44] with a jet resolution parameter $y_{cut} = 0.006$. To determine the thrust axis of the event we also use calorimeter clusters.

4. Bose-Einstein Correlation Function

The two-particle Bose-Einstein correlation function is given by (1) or (2). In these equations, ρ_2 is corrected for detector acceptance and efficiency using Monte Carlo events, to which a full detector simulation has been applied, on a bin-by-bin basis. An event mixing technique is used to construct ρ_0. This technique removes all correlations, not just Bose-Einstein. Hence, ρ_0 is corrected for this using Monte Carlo.[41]

Since Bose-Einstein correlations can be large only at small four-momentum difference Q, they are often parametrized in this one-dimensional distance measure. There is no reason, however, to expect the hadron source to be spherically symmetric in jet fragmentation. As stated above (Sect. 2.6), an elongation of the source along the jet axis[10,15,31,32] has been observed. While this effect is well established, the elongation is actually only about 20%, which suggests that a parametrization in terms of the single variable Q, may be a good approximation.

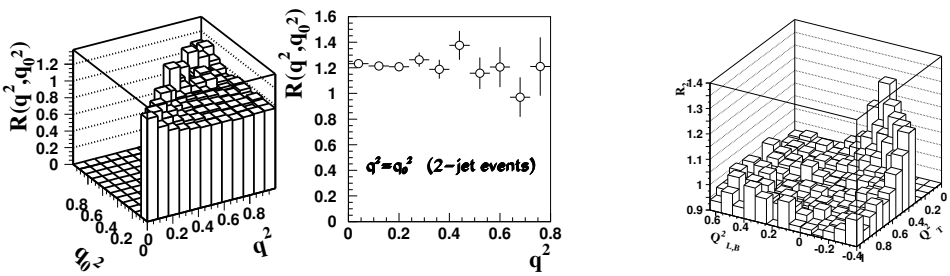

Fig. 4. For two-jet events: (a) R_2 as function of the squares of the 3-momentum difference, q, and the energy difference, q_0; (b) R_2 *vs.* q^2 when $q^2 \approx q_0^2$; and (c) R_2 as function of the squares of the transverse momentum difference and the combination of longitudinal momentum difference and energy difference.

This is not the case in heavy-ion and hadron-hadron interactions, where BEC are found not to depend simply on Q, but on components of the momentum difference separately.[5,45–48] However, in e^+e^- annihilation at lower energy[18] it has been observed that Q is the appropriate variable. We checked this and confirm that this is indeed the case: We observe (see Fig. 4 that R_2 does not decrease when both $q^2 = (\vec{p}_1 - \vec{p}_2)^2$ and $q_0^2 = (E_1 - E_2)^2$ are large while $Q^2 = q^2 - q_0^2$ is small, but is maximal for $Q^2 = q^2 - q_0^2 = 0$, independent of the individual values of q and q_0. The same is observed in a different decomposition: $Q^2 = Q_{\rm t}^2 + Q_{L,B}^2$, where $Q_{\rm t}^2 = (\vec{p}_{\rm t1} - \vec{p}_{\rm t2})^2$ is the component transverse to the thrust axis and $Q_{L,B}^2 = (p_{\rm l1} - p_{\rm l2})^2 - (E_1 - E_2)^2$ combines the longitudinal momentum and energy differences. Again, R_2 is maximal along the line $Q = 0$, as is also shown in Fig. 4. This is observed both for two-jet and three-jet events. We conclude that a parametrization in terms of Q can be considered a good approximation for the purposes of this article.

5. Parametrizations of BEC

With a few assumptions,[2,5,6] the two-particle correlation function, (1), is related to the Fourier transformed source distribution:

$$R_2(p_1, p_2) = \gamma \left[1 + \lambda |\tilde{f}(Q)|^2\right] (1 + \delta Q) \ , \tag{4}$$

where $f(x)$ is the (configuration space) density distribution of the source, and $\tilde{f}(Q)$ is the Fourier transform (characteristic function) of $f(x)$. The parameter γ and the $(1 + \delta Q)$ term have been introduced to parametrize possible long-range correlations not adequately accounted for in the reference sample, and the parameter λ to account for several factors, such as the possible lack of complete incoherence of particle production and the presence of long-lived resonance decays if the particle emission consists of a small, resolvable core and a halo with experimentally unresolvable large length scales.[49,50]

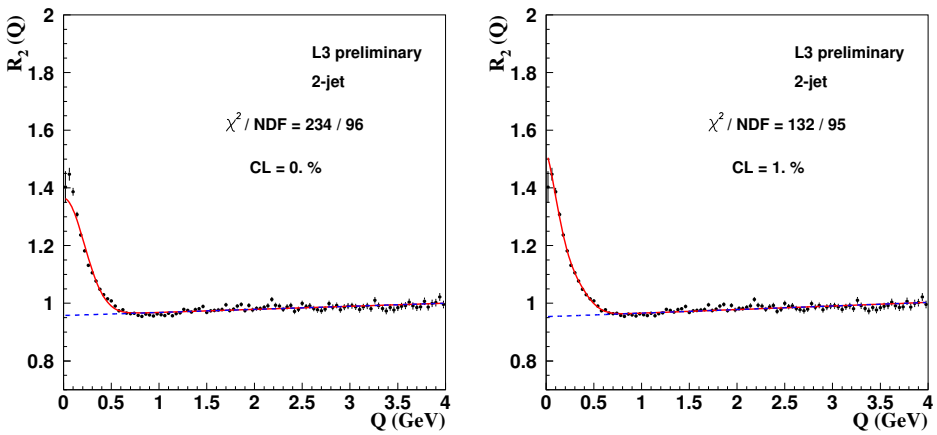

Fig. 5. The Bose-Einstein correlation function R_2 for two-jet events with the result of a fit of (left) the Gaussian and (right) the Edgeworth parametrizations, (5) and (6), respectively. The dashed line represents the long-range part of the fit, *i.e.*, $\gamma(1+\delta Q)$.

5.1. *Gaussian distributed source*

The simplest assumption is that the source has a symmetric Gaussian distribution, in which case $\tilde{f}(Q) = \exp\left(i\mu Q - \frac{(rQ)^2}{2}\right)$ and

$$R_2(Q) = \gamma\left[1 + \lambda \exp\left(-(rQ)^2\right)\right](1+\delta Q) \ . \tag{5}$$

A fit of (5) to the data results in an unacceptably low confidence level. The fit is particularly bad at low Q values, as is shown in Fig. 5a for two-jet events and in Fig. 6a for three-jet events, from which we conclude that the shape of the source deviates from a Gaussian.

A model-independent way to study deviations from the Gaussian parametrization is to use[5,51,52] the Edgeworth expansion[7] about a Gaussian. Keeping only the first non-Gaussian term, we have

$$R_2(Q) = \gamma\left(1 + \lambda \exp\left(-(rQ)^2\right)\left[1 + \frac{\kappa}{3!}H_3(rQ)\right]\right)(1+\delta Q) \ , \tag{6}$$

where κ is the third-order cumulant moment and $H_3(rQ) \equiv (\sqrt{2}rQ)^3 - 3\sqrt{2}rQ$ is the third-order Hermite polynomial. Note that the second-order cumulant corresponds to the radius r.

A fit of (6) to the two-jet data, shown in Fig. 5b, is indeed much better than the purely Gaussian fit, and the departure from a Gaussian is highly significant: $\kappa = 0.71 \pm 0.06$. However, the confidence level is still marginal, and close inspection of the figure shows that the fit curve is systematically above the data in the region 0.6–1.2 GeV and that the data for $Q \geq 1.5$ GeV appear flatter than the curve, as is also the case for the purely Gaussian fit. Similar behavior is observed for three-jet events (Fig. 6b).

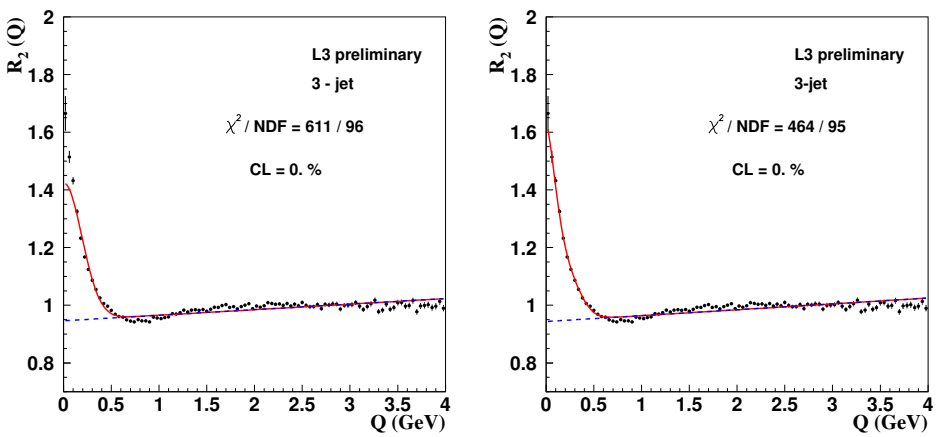

Fig. 6. The Bose-Einstein correlation function R_2 for three-jet events with the result of a fit of (left) the Gaussian and (right) the Edgeworth parametrizations, (5) and (6), respectively. The dashed line represents the long-range part of the fit, *i.e.*, $\gamma(1+\delta Q)$.

5.2. *Lévy distributed source*

The symmetric Lévy stable distribution is characterized by three parameters: x_0, r, and α. Its Fourier transform, $\tilde{f}(Q)$, has the following form:

$$\tilde{f}(Q) = \exp\left(iQx_0 - \frac{|rQ|^\alpha}{2}\right) . \tag{7}$$

The index of stability, α, satisfies the inequality $0 < \alpha \leq 2$. The case $\alpha = 2$ corresponds to a Gaussian source distribution with mean x_0 and standard deviation r. For more details, see, *e.g.*, Ref. 53.

Then R_2 has the following, relatively simple, form:[54]

$$R_2(Q) = \gamma\left[1 + \lambda \exp\left(-(rQ)^\alpha\right)\right](1+\delta Q) . \tag{8}$$

From the fit of (8) to the two-jet data, shown in Fig. 7, it is clear that the correlation function is far from Gaussian: $\alpha = 1.34 \pm 0.04$. The confidence level, although improved compared to the fit of (5), is still unacceptably low, in fact worse than that for the Edgeworth parametrization. The same is true for three-jet events (Fig. 7).

Both the symmetric Lévy parametrization and the Edgeworth parametrizations do a fair job of describing the region $Q < 0.6\,\text{GeV}$, but fail at higher Q. In the region $Q \geq 1.5\,\text{GeV}$, R_2 is nearly constant (≈ 1). However, in the region 0.6–1.5 GeV R_2 has a smaller value, dipping below unity,[a] which is indicative of an anti-correlation. This is clearly seen in Fig. 7 by comparing the data in this region to an extrapolation of a linear fit, (8) with $\lambda = 0$, in the region $Q \geq 1.5\,\text{GeV}$. The inability to describe this dip in R_2 is the primary reason for the failure of both the Edgeworth and symmetric Lévy parametrizations.

[a]More correctly, dipping below the value of the parameter γ.

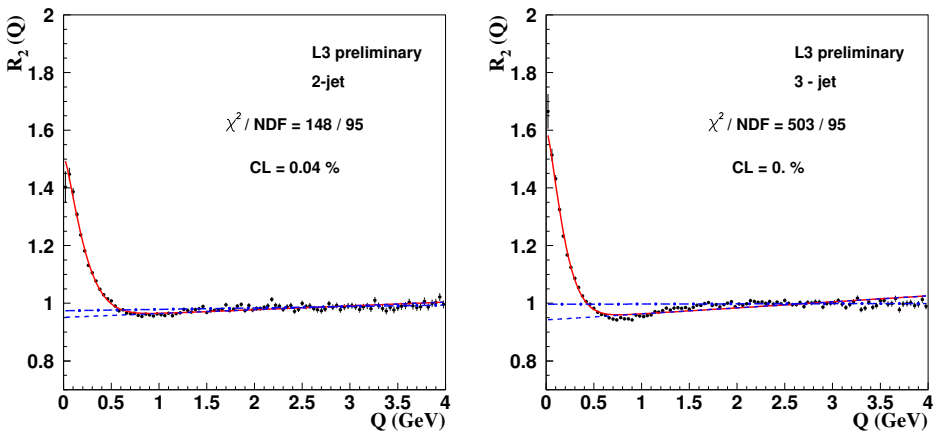

Fig. 7. The Bose-Einstein correlation function R_2 for two-jet events (left) and for three-jet events (right). The curve corresponds to the fit of the symmetric Lévy parametrization, (8). The dashed line represents the long-range part of the fit, *i.e.*, $\gamma(1+\delta Q)$. The dot-dashed line represents a linear fit in the region $Q > 1.5\,\mathrm{GeV}$.

5.3. *Time dependence of the source*

The parametrizations discussed so far, which have proved insufficient to describe the BEC, all assume a static source. The parameter r, representing the size of the source as seen in the rest frame of the pion pair, is a constant. It has, however, been observed that r depends on the transverse mass, $m_\mathrm{t} = \sqrt{m^2 + p_\mathrm{t}^2} = \sqrt{E^2 - p_z^2}$, of the pions.[34,35] It has been shown[55,56] that this dependence can be understood if the produced pions satisfy, approximately, the (generalized) Bjorken-Gottfried condition,[57–62] whereby the four-momentum of a produced particle and the space-time position at which it is produced are linearly related:

$$x^\mu = dk^\mu \ . \tag{9}$$

Such a correlation between space-time and momentum-energy is also a feature of the Lund string model as incorporated in JETSET, which is very successful in describing detailed features of the hadronic final states of $\mathrm{e^+e^-}$ annihilation.

In the previous section we have seen that BEC depend, at least approximately, only on Q and not on its components separately. This is a non-trivial result. For a hydrodynamical type of source, on the contrary, BEC decrease when any of the relative momentum components is large.[5,45] Further, we have seen that R_2 in the region 0.6–1.5 GeV dips below its values at higher Q.

A model which predicts such Q-dependence while incorporating the Bjorken-Gottfried condition is the so-called τ-model, described below.

5.3.1. *The τ-model*

A model of strongly correlated phase-space, known as the τ-model,[63] explains the experimental observation that BEC in e^+e^- reactions depend only on Q rather than on the components of Q separately. This model also predicts a specific transverse mass dependence of R_2, which we subject to an experimental test here.

In this model, it is assumed that the average production point in the overall center-of-mass system, $\overline{x} = (\overline{t}, \overline{r}_x, \overline{r}_y, \overline{r}_z)$, of particles with a given four-momentum k is given by

$$\overline{x}^\mu(k^\mu) = dk^\mu \ . \tag{10}$$

In the case of two-jet events,

$$d = \tau/m_{\rm t} \ , \tag{11}$$

where $m_{\rm t}$ is the transverse mass and $\tau = \sqrt{\overline{t}^2 - \overline{r}_z^2}$ is the longitudinal proper time.[b] For isotropically distributed particle production, the transverse mass is replaced by the mass in (11), while for the case of three-jet events the relation is more complicated. The second assumption is that the distribution of $x^\mu(k^\mu)$ about its average, $\delta_\Delta(x^\mu(k^\mu) - \overline{x}^\mu(k^\mu))$, is narrower than the proper-time distribution. Then the emission function of the τ-model is

$$S(x,k) = \int_0^\infty {\rm d}\tau H(\tau)\delta_\Delta(x - dk)\rho_1(k) \ , \tag{12}$$

where $H(\tau)$ is the longitudinal proper-time distribution, the factor $\delta_\Delta(x - dk)$ describes the strength of the correlations between coordinate space and momentum space variables and $\rho_1(k)$ is the experimentally measurable single-particle spectrum.

The two-pion distribution, $\rho_2(k_1, k_2)$, is related to $S(x,k)$, in the plane-wave approximation, by the Yano-Koonin formula:[64]

$$\begin{aligned}\rho_2(k_1,k_2) = \int & {\rm d}^4x_1{\rm d}^4x_2 S(x_1,k_1)S(x_2,k_2) \\ & \cdot \big(1 + \cos\big([k_1 - k_2]\,[x_1 - x_2]\big)\big) \ .\end{aligned} \tag{13}$$

Approximating the function δ_Δ by a Dirac delta function, the argument of the cosine becomes

$$(k_1 - k_2)(\bar{x}_1 - \bar{x}_2) = -0.5(d_1 + d_2)Q^2 \ . \tag{14}$$

Then the two-particle Bose-Einstein correlation function is approximated by

$$R_2(k_1,k_2) = 1 + \lambda {\rm Re}\widetilde{H}^2\left(\frac{Q^2}{2\overline{m}_{\rm t}}\right) \ , \tag{15}$$

[b]The terminology 'longitudinal' proper time and 'transverse' mass seems customary in the literature even though their definitions are analogous $\tau = \sqrt{\overline{t}^2 - \overline{r}_z^2}$ and $m_{\rm t} = \sqrt{E^2 - p_z^2}$.

where $\widetilde{H}(\omega) = \int \mathrm{d}\tau H(\tau) \exp(i\omega\tau)$ is the Fourier transform of $H(\tau)$. Thus an invariant relative momentum dependent BEC appears. Note that R_2 depends not only on Q but also on the average transverse mass of the two pions, $\overline{m}_\mathrm{t}$.

Since there is no particle production before the onset of the collision, $H(\tau)$ should be a one-sided distribution. We choose a one-sided Lévy distribution, which has the characteristic function[54] (for $\alpha \neq 1$)

$$\widetilde{H}(\omega) = \exp\left[-\frac{1}{2}\left(\Delta\tau|\omega|\right)^\alpha \left(1 - i\,\mathrm{sign}(\omega)\tan\left(\frac{\alpha\pi}{2}\right)\right) + i\,\omega\tau_0\right] \tag{16}$$

where the parameter τ_0 is the proper time of the onset of particle production and $\Delta\tau$ is a measure of the width of the proper-time distribution. For the special case $\alpha = 1$, see, *e.g.*, Ref. 53. Using this characteristic function in (15) yields

$$R_2(Q, \overline{m}_\mathrm{t}) = \gamma\left[1 + \lambda\cos\left(\frac{\tau_0 Q^2}{\overline{m}_\mathrm{t}} + \tan\left(\frac{\alpha\pi}{2}\right)\left(\frac{\Delta\tau Q^2}{2\overline{m}_\mathrm{t}}\right)^\alpha\right)\right.$$
$$\left.\cdot\exp\left(-\left(\frac{\Delta\tau Q^2}{2\overline{m}_\mathrm{t}}\right)^\alpha\right)\right](1 + \delta Q)\,. \tag{17}$$

5.3.2. *The τ-model for average m_t*

Before proceeding to fits of (17), we first consider a simplification of the equation obtained by assuming (a) that particle production starts immediately, *i.e.*, $\tau_0 = 0$, and (b) an average m_t dependence, which is implemented in an approximate way by defining an effective radius, $R = \sqrt{\Delta\tau/(2\overline{m}_\mathrm{t})}$. This results in:

$$R_2(Q) = \gamma\left[1 + \lambda\cos\left[(R_\mathrm{a}Q)^{2\alpha}\right]\exp\left(-(RQ)^{2\alpha}\right)\right](1 + \delta Q)\,, \tag{18}$$

where R_a is related to R by

$$R_\mathrm{a}^{2\alpha} = \tan\left(\frac{\alpha\pi}{2}\right)R^{2\alpha}\,. \tag{19}$$

Fits of (18) are first performed with R_a as a free parameter. The fit results obtained, for two-jet, three-jet, and all events are listed in Table 1 and shown in Fig. 8 for two-jet events and for three-jet events. They have acceptable confidence levels, describing well the dip below unity in the 0.6–1.5 GeV region, as well as the low-Q peak.

The fit parameters for the two-jet events satisfy (19). However, those for three-jet and all events do not. We note that the values of the parameters α and R do not differ greatly between 2- and 3-jet samples, the most significant difference appearing to be nearly 3σ for α. However, these parameters are rather highly correlated (in the fit for all events, the correlation coefficients are $\rho(\lambda, R) = 0.95$, $\rho(\lambda, \alpha) = -0.67$ and $\rho(R, \alpha) = -0.61$, which makes the simple calculation of the statistical significance of differences in the parameters unreliable.

Fit results imposing (19) are given in Table 2. For two-jet events, the values of the parameters are nearly identical to those in the fit with R_a free—only the uncertainties have changed. For three-jet and all events, the imposition of (19)

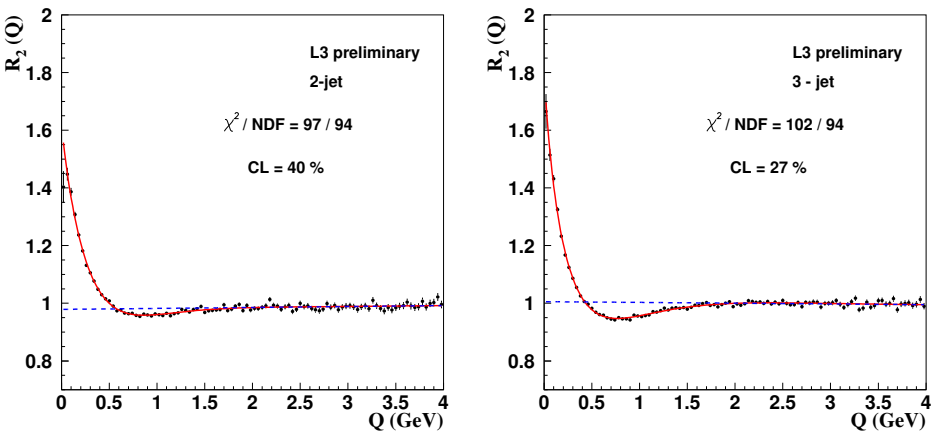

Fig. 8. The Bose-Einstein correlation function R_2 for two-jet events (left) and for three-jet events (right). The curve corresponds to the fit of the one-sided Lévy parametrization, (18). The dashed line represents the long-range part of the fit, *i.e.*, $\gamma(1+\delta Q)$.

Table 1. Results of fits of (18) for two-jet, three-jet, and all events. The uncertainties are only statistical.

parameter	2-jet	3-jet	all
α	0.42 ± 0.02	0.35 ± 0.01	0.38 ± 0.01
λ	0.67 ± 0.03	0.84 ± 0.04	0.73 ± 0.02
R (fm)	0.79 ± 0.04	0.89 ± 0.03	0.81 ± 0.03
$R_{\rm a}$ (fm)	0.59 ± 0.03	0.88 ± 0.04	0.81 ± 0.02
δ	0.003 ± 0.002	-0.003 ± 0.002	0.003 ± 0.001
γ	0.979 ± 0.005	1.001 ± 0.005	0.997 ± 0.003
χ^2/DoF	97/94	102/94	98/94
confidence level	40%	27%	37%

results in values of α and R closer to those for two-jet events, but the confidence levels are very bad, a consequence of incompatibility with (19), an incompatibility that is not surprizing given that (11) is only valid for two-jet events. Therefore, we only consider two-jet events in the remaining sections of this article.

5.3.3. *The τ-model with $m_{\rm t}$ dependence*

Fits of (17) to the two-jet data are performed in several $m_{\rm t}$ intervals. The resulting fits are shown for several $m_{\rm t}$ intervals in Fig. 9, and the values of the parameters obtained in the fits are displayed in Fig. 10. The quality of the fits is seen to be statistically acceptable and the fitted values of the model parameters, α, τ_0 and $\Delta\tau$, are stable and within errors independent of $m_{\rm t}$, confirming the expectation of the τ-model. We conclude that the τ-model with a one-sided Levy proper-time

Table 2. Results of fits of (18) imposing (19) for two-jet, three-jet, and all events. The uncertainties are only statistical.

parameter	2-jet	3-jet	all
α	0.42 ± 0.01	0.44 ± 0.01	0.45 ± 0.01
λ	0.67 ± 0.03	0.77 ± 0.04	0.69 ± 0.03
R (fm)	0.79 ± 0.03	0.84 ± 0.04	0.79 ± 0.03
δ	0.003 ± 0.001	0.010 ± 0.001	0.009 ± 0.001
γ	0.979 ± 0.005	0.972 ± 0.001	0.973 ± 0.001
χ^2/DoF	97/95	174/95	175/95
confidence level	42%	10^{-6}	10^{-6}

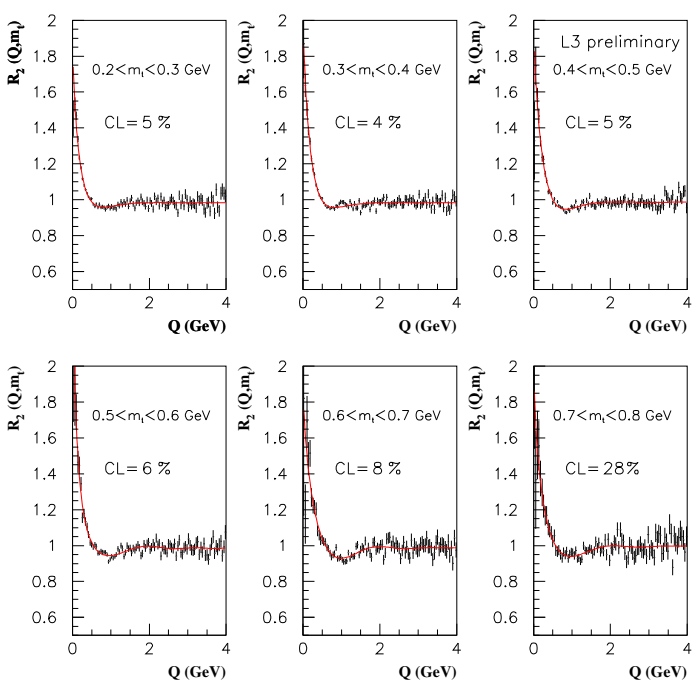

Fig. 9. The results of fits of (17) to two-jet data for various intervals of $m_{\rm t}$.

distribution describes the data with parameters $\tau_0 \approx 0$ fm, $\alpha \approx 0.38 \pm 0.05$ and $\Delta\tau \approx 3.5 \pm 0.6$ fm. These values are consistent with the fit of (18) in the previous section, including the value of R, which, combined with the average value of $m_{\rm t}$ (0.563 GeV), corresponds to $\Delta\tau = 3.5$ fm. Just as in the fit of (18), the parameters of the Lévy distribution are highly correlated. Typical values of the correlation coefficients are $\rho(\lambda, \Delta\tau) = 0.95$, $\rho(\lambda, \alpha) = -0.67$ and $\rho(\Delta\tau, \alpha) = -0.9$.

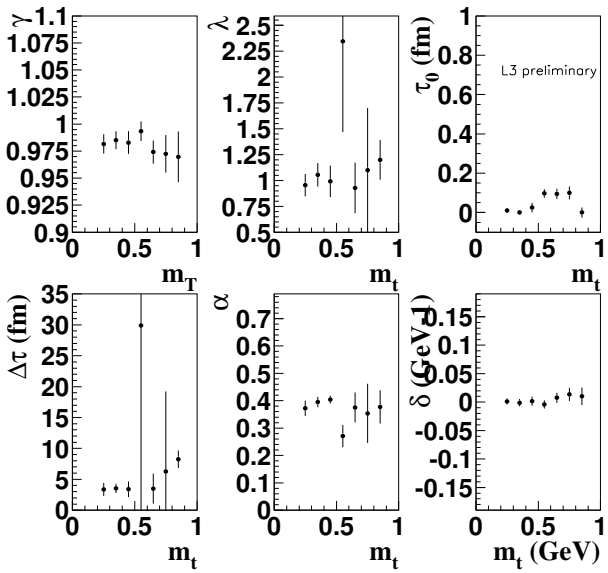

Fig. 10. The fit parameters from fits of (17) to two-jet data for various intervals of $m_{\rm t}$.

6. The emission function of two-jet events

Within the framework of the τ-model, we now reconstruct the space-time picture of the emitting process for two-jet events. The emission function in configuration space, $S(x)$, is the proper time derivative of the integral over k of $S(x,k)$, which in the τ-model is given by (12). Approximating δ_Δ by a Dirac delta function, we find

$$S(x) = \frac{\mathrm{d}^4 n}{\mathrm{d}\tau \mathrm{d}^3 r} = \left(\frac{m_{\rm t}}{\tau}\right)^3 H(\tau)\rho_1\left(k = \frac{m_{\rm t} r}{\tau}\right) \ . \tag{20}$$

To simplify the reconstruction of $S(x)$ we assume that it can be factorized in the following way:

$$S(r_{\rm t}, z, t) = I(r_{\rm t})G(\eta)H(\tau) \ , \tag{21}$$

where $I(r_{\rm t})$ is the single-particle transverse distribution, $G(\eta)$ is the space-time rapidity distribution of particle production, and $H(\tau)$ is the proper-time distribution. With the strongly correlated phase-space of the τ-model, $\eta = y$ and $r_{\rm t} = p_{\rm t}\tau/m_{\rm t}$. Hence,

$$G(\eta) = N_y(\eta) \ , \tag{22}$$

$$I(r_{\rm t}) = \left(\frac{m_{\rm t}}{\tau}\right)^3 N_{p_{\rm t}}(r_{\rm t} m_{\rm t}/\tau) \ , \tag{23}$$

where N_y and $N_{p_{\rm t}}$ are the single-particle inclusive rapidity and $p_{\rm t}$ distributions, respectively. The factorization of transverse and longitudinal distributions has been checked. The distribution of $p_{\rm t}$ is, to a good approximation, independent of the rapidity.[41]

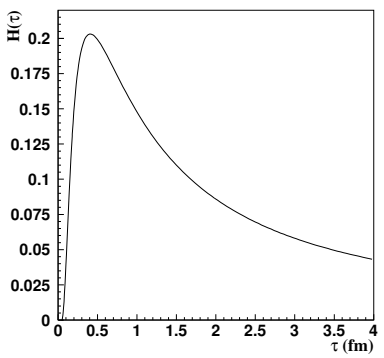

Fig. 11. The proper time distribution, $H(\tau)$, for $\alpha = 0.4$, $\tau_0 = 0$ and $\Delta\tau = 3.5\,\mathrm{fm}$.

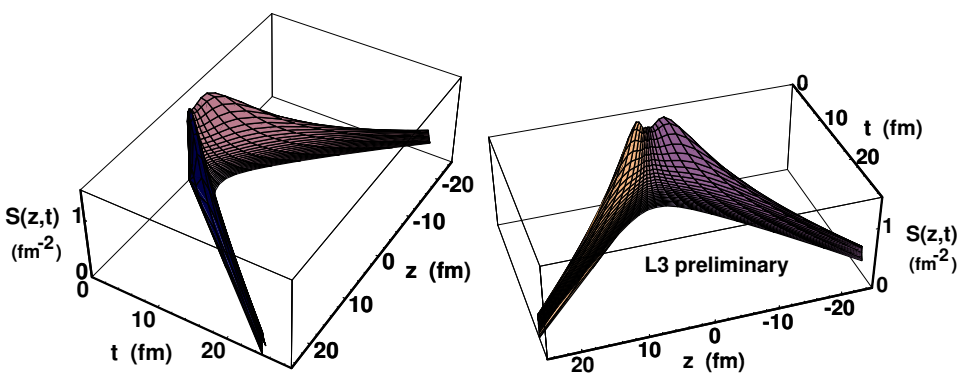

Fig. 12. Two views of the temporal-longitudinal part of the source function normalized to the average number of pions per event.

With these assumptions and using $H(\tau)$ as obtained from the fit of (17) (shown in Fig. 11) together with the inclusive rapidity and p_{t} distributions,[41] the full emission function is reconstructed. Its integral over the transverse distribution is plotted in Fig. 12. It exhibits a "boomerang" shape with a maximum at low t and z but with tails reaching out to very large values of t and z, a feature also observed in hadron-hadron[65] and heavy ion collisions.[66]

The transverse part of the emission function is obtained by integrating over z and azimuthal angle. Fig. 13 shows the transverse part of the emission function for various proper times. Particle production starts immediately, increases rapidly and decreases slowly. A ring-like structure, similar to the expanding, ring-like wave created by a pebble in a pond, is observed. These pictures together form a movie that ends in about 3.5 fm, making it the shortest movie ever made of a process in nature. An animated gif file covering the first 0.3 fm (10^{-24} sec) is available.[67]

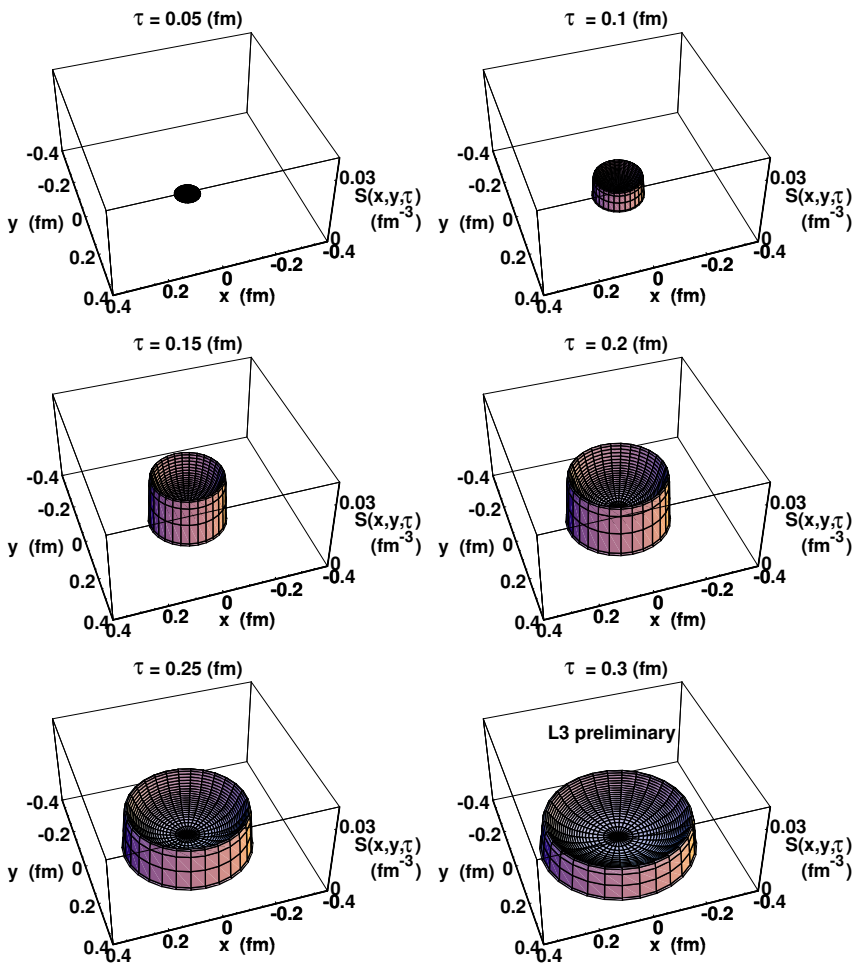

Fig. 13. The transverse source function normalized to the average number of pions per event for various proper times.

7. Discussion

BEC of all events as well as two- and three-jet events are observed to be well-described by a Lévy parametrization incorporating strong correlations between configuration- and momentum-space. A Lévy distribution arises naturally from a fractal, or from a random walk or anomalous diffusion,[68] and the parton shower of the leading log approximation of QCD is a fractal.[69–72] In this case, the Lévy index of stability is related to the strong coupling constant, α_s, by[73,74]

$$\alpha_s = \frac{2\pi}{3}\alpha^2 \ . \tag{24}$$

Assuming (generalized) local parton hadron duality,[75–77] one can expect that the distribution of hadrons retains the features of the gluon distribution. For the value of α found in fits of (18) we find $\alpha_{\rm s} = 0.37 \pm 0.04$ for two-jet events, This is a reasonable value for a scale of 1–2 GeV, which is where the production of hadrons takes place. For comparison, from τ decay, $\alpha_{\rm s}(m_\tau \approx 1.8\,{\rm GeV}) = 0.35 \pm 0.03$.[78]

It is of particular interest to point out the $m_{\rm t}$ dependence of the "width" of the source. In (17) the parameter associated with the width is $\Delta\tau$. Note that it enters (17) as $\Delta\tau Q^2/\overline{m}_{\rm t}$. In a Gaussian parametrization the radius r enters the parametrization as r^2Q^2. Our observance that $\Delta\tau$ is independent of $\overline{m}_{\rm t}$ thus corresponds to $r \propto 1/\sqrt{\overline{m}_{\rm t}}$ and can be interpreted as confirmation of the observance[34, 35] of such a dependence of the Gaussian radii in 2- and 3-dimensional analyses of Z decays. The lack of dependence of all the parameters of (17) on the transverse mass is in accordance with the τ-model.

Using the BEC fit results and the τ-model, the emission function of two-jet events is reconstructed. Particle production begins immediately after collision, increases rapidly and then decreases slowly, occuring predominantly close to the light cone. In the transverse plane a ring-like structure expands outwards, which is similar to the picture in hadron-hadron interactions but unlike that of heavy ion collisions.

References

1. M. Gyulassy, S.K. Kauffmann and Lance W. Wilson, Phys. Rev. **C20** (1979) 2267–2292.
2. David H. Boal, Claus-Konrad Gelbke and Byron K. Jennings, Rev. Mod. Phys. **62** (1990) 553–602.
3. Gordon Baym, Acta Phys. Pol. **B29** (1998) 1839–1884.
4. W. Kittel, Acta Phys. Pol. **B32** (2001) 3927–3972.
5. T. Csörgő, Heavy Ion Physics **15** (2002) 1–80.
6. Gerson Goldhaber, Sulamith Goldhaber, Wonyong Lee and Abraham Pais, Phys. Rev. **120** (1960) 300–312.
7. F.Y. Edgeworth, Trans. Cambridge Phil. Soc. **20** (1905) 36, see also, *e.g.*, Harald Cramér, Mathematical Methods of Statistics, (Princeton Univ. Press, 1946).
8. W.J. Metzger, Bose-Einstein Correlations in e^+e^- Annihilation and $e^+e^- \to W^+W^-$, E-print hep-ph/0509031, 2005.
9. ALEPH Collab., D. Decamp *et al.*, Z. Phys. **C54** (1992) 75–85.
10. ALEPH Collab., A. Heister *et al.*, Eur. Phys. J. **C36** (2004) 147–159.
11. DELPHI Collab., P. Abreu *et al.*, Phys. Lett. **B286** (1992) 201–210.
12. L3 Collab., P. Achard *et al.*, Phys. Lett. **B540** (2002) 185–198.
13. OPAL Collab., P.D. Acton *et al.*, Phys. Lett. **B267** (1991) 143–153.
14. OPAL Collab., G. Alexander *et al.*, Z. Phys. **C72** (1996) 389–398.
15. OPAL Collab., G. Abbiendi *et al.*, Eur. Phys. J. **C16** (2000) 423–433.
16. H. Aihara *et al.*, Phys. Rev. **D31** (1985) 996–1003.
17. I. Juricic *et al.*, Phys. Rev. **D39** (1989) 1–20.
18. TASSO Collab., M. Althoff *et al.*, Z. Phys. **C30** (1986) 355–369.
19. AMY Collab., S.K. Choi *et al.*, Phys. Lett. **B355** (1995) 406–414.
20. Gideon Alexander, Rep. Prog. Phys. **66** (2003) 481–522.
21. Gösta Gustafson, Fluctuations and Fermi-Dirac Correlations in e^+e^--annihilation, E-print hep-ph/0611296, 2006.
22. DELPHI Collab., P. Abreu *et al.*, Phys. Lett. **B379** (1996) 330–340.
23. OPAL Collab., G. Abbiendi *et al.*, Eur. Phys. J. **C21** (2001) 23–32.
24. ALEPH Collab., S. Schael *et al.*, Phys. Lett. **B611** (2005) 66–80.
25. OPAL Collab., R. Akers *et al.*, Z. Phys. **C67** (1995) 389–401.
26. ALEPH Collab., R. Barate *et al.*, Phys. Lett. **B475** (2000) 395–406.
27. OPAL Collab., G. Alexander *et al.*, Phys. Lett. **B384** (1996) 377–387.
28. Bo Andersson and Werner Hofmann, Phys. Lett. **B169** (1986) 364–368.
29. Bo Andersson and Markus Ringnér, Nucl. Phys. **B513** (1998) 627–644.
30. Bo Andersson and Markus Ringnér, Phys. Lett. **B421** (1998) 283–288.
31. L3 Collab., M. Acciarri *et al.*, Phys. Lett. **B458** (1999) 517–528.
32. DELPHI Collab., P. Abreu *et al.*, Phys. Lett. **B471** (2000) 460–470.
33. ZEUS Collab., S. Chekanov *et al.*, Phys. Lett. **B583** (2004) 231–246.
34. B. Lörstad and O.G. Smirnova, in Proc. 7th Int. Workshop on Multiparticle Production "Correlations and Fluctuations", ed. R.C. Hwa *et al.*, (World Scientific, Singapore, 1997), p. 42.
35. J.A. van Dalen, in Proc. 8th Int. Workshop on Multiparticle Production "Correlations and Fluctuations '98: From QCD to Particle Interferometry", ed. T. Csörgő *et al.*, (World Scientific, Singapore, 1999), p. 37.
36. L3 Collab., B. Adeva *et al.*, Nucl. Inst. Meth. **A 289** (1990) 35–102.
37. J.A. Bakken *et al.*, Nucl. Inst. Meth. **A 275** (1989) 81–88.
38. O. Adriani *et al.*, Nucl. Inst. Meth. **A 302** (1991) 53–62.
39. K. Deiters *et al.*, Nucl. Inst. Meth. **A 323** (1992) 162–168.

40. M. Acciarri *et al.*, Nucl. Inst. Meth. **A 351** (1994) 300–312.
41. Tamás Novák, Ph.D. thesis, Radboud Univ. Nijmegen, *in preparation*.
42. Yu.L. Dokshitzer, Contribution cited in Report of the Hard QCD Working Group, Proc. Workshop on Jet Studies at LEP and HERA, Durham, Dec. 1990, J. Phys. G17 (1991) 1537.
43. S. Catani *et al.*, Phys. Lett. **B269** (1991) 432–438.
44. S. Bethke *et al.*, Nucl. Phys. **B370** (1992) 310–334.
45. T. Csörgő and B. Lörstadt, Phys. Rev. **C54** (1996) 1390–1403.
46. NA22 Collab., N.M. Agababyan *et al.*, Z. Phys. **C71** (1996) 405–414.
47. Ron A. Solz, Two-Pion Correlation Measurements for 14.6A·GeV/c ^{28}Si+X and 11.6A·GeV/c ^{197}Au+Au, Ph.D. thesis, Massachusetts Inst. of Technology., 1994.
48. E-802 Collab., L. Ahle *et al.*, Phys. Rev. **C66** (2002) 054906–1–15.
49. J. Bolz *et al.*, Phys. Rev. **D47** (1993) 3860–3870.
50. T. Csörgő, B. Lörstad and J. Zimányi, Z. Phys. **C71** (1996) 491–497.
51. T. Csörgő and S. Hegyi, in Proc. XXVIIIth Rencontres de Moriond, ed. Étienne Augé and J. Trân Thanh Vân, (Editions Frontières, Gif-sur-Yvette, France, 1993), p. 635.
52. T. Csörgő, in Proc. Cracow Workshop on Multiparticle Production, ed. A. Białas *et al.*, (World Scientific, Singapore, 1994), p. 175.
53. J.P. Nolan, Stable distributions: Models for Heavy Tailed Data, 2005, `http://academic2.american.edu/~jpnolan/stable/CHAP1.PDF`.
54. T. Csörgő, S. Hegyi and W.A. Zajc, Eur. Phys. J. **C36** (2004) 67–78.
55. A. Białas and K. Zalewski, Acta Phys. Pol. **B30** (1999) 359–367.
56. A. Białas *et al.*, Phys. Rev. **D62** (1999) 114007–1–7.
57. K. Gottfried, Acta Phys. Pol. **B3** (1972) 769.
58. J.D. Bjorken, in Proc. Summer Inst. on Particle Physics, Vol. 1, (SLAC-R-167, 1973), pp. 1–34.
59. J.D. Bjorken, Phys. Rev. **D7** (1973) 282–283.
60. K. Gottfried, Phys. Rev. Lett. **32** (1974) 957–961.
61. F.E. Low and K. Gottfried, Phys. Rev. **D17** (1978) 2487–2491.
62. J.D. Bjorken, in Proc. XXIV Int. Symp. on Multiparticle Dynamics, ed. A. Giovannini *et al.*, (World Scientific, Singapore, 1995), p. 579.
63. T. Csörgő and J. Zimányi, Nucl. Phys. **A517** (1990) 588–598.
64. F.B. Yano and S.E. Koonin, Phys. Lett. **B78** (1978) 556–559.
65. NA22 Collab., N.M. Agababyan *et al.*, Phys. Lett. **B422** (1998) 359–368.
66. A. Ster, T. Csörgő and B. Lörstad, Nucl. Phys. **A661** (1999) 419–422.
67. T. Novák, `http://www.hef.ru.nl/~novakt/movie/movie.gif`.
68. R. Metzler and J. Klafter, Phys. Rep. **339** (2000) 1–77.
69. P. Dahlqvist, B. Andersson and G. Gustafson, Nucl. Phys. **B328** (1989) 76.
70. G. Gustafson and A. Nilsson, Nucl. Phys. **B355** (1991) 106.
71. G. Gustafson and A. Nilsson, Z. Phys. **C52** (1991) 533.
72. Yu.L. Dokshitzer and I.M. Dremin, Nucl. Phys. **B402** (1993) 139–165.
73. T. Csörgő *et al.*, Acta Phys. Pol. **B36** (2005) 329–337.
74. T. Csörgő *et al.*, Bose-Einstein or HBT correlation signature of a second order QCD phase transition, 2005, `http://arXiv.org/abs/nucl-th/0512060`.
75. Ya.I. Azimov *et al.*, Z. Phys. **C27** (1985) 65–72.
76. Ya.I. Azimov *et al.*, Z. Phys. **C31** (1986) 213–218.
77. L. Van Hove and A. Giovannini, Acta Phys. Pol. **B19** (1988) 931–946.
78. Particle Data Group, S. Eidelman *et al.*, Phys. Lett. **B592** (2004) 1–1109.